Cite as: L. Amoasii *et al.*, *Science* 10.1126/aau1549 (2018).

Gene editing restores dystrophin expression in a canine model of Duchenne muscular dystrophy

Leonela Amoasii[1,2], John C.W. Hildyard[3], Hui Li[1], Efrain Sanchez-Ortiz[1], Alex Mireault[1], Daniel Caballero[1], Rachel Harron[3], Thaleia-Rengina Stathopoulou[4], Claire Massey[3], John M. Shelton[5], Rhonda Bassel-Duby[1], Richard J. Piercy[3], Eric N. Olson[1]*

[1]Department of Molecular Biology, Hamon Center for Regenerative Science and Medicine, Sen. Paul D. Wellstone Muscular Dystrophy Cooperative Research Center, University of Texas Southwestern Medical Center, 5323 Harry Hines Boulevard, Dallas, TX 75390, USA. [2]Exonics Therapeutics, 75 Kneeland Street, Boston, MA 02111, USA. [3]Department of Clinical Science and Services, Comparative Neuromuscular Diseases Laboratory, Royal Veterinary College, London NW1 0TU, UK. [4]Section of Anaesthesia and Analgesia, Royal Veterinary College, London NW1 0TU, UK. [5]Department of Internal Medicine, University of Texas Southwestern Medical Center, 5323 Harry Hines Boulevard, Dallas, TX 75390, USA.

*Corresponding author. Email: eric.olson@utsouthwestern.edu

Mutations in the gene encoding dystrophin, a protein that maintains muscle integrity and function, cause Duchenne muscular dystrophy (DMD). The deltaE50-MD dog model of DMD harbors a mutation corresponding to a mutational "hot spot" in the human *DMD* gene. We used adeno-associated viruses to deliver CRISPR gene editing components to four dogs and examined dystrophin protein expression 6 weeks after intramuscular delivery (n=2) or 8 weeks after systemic delivery (n=2). After systemic delivery in skeletal muscle, dystrophin was restored to levels ranging from 3 to 90% of normal, depending on muscle type. In cardiac muscle, dystrophin levels in the dog receiving the highest dose reached 92% of normal. The treated dogs also showed improved muscle histology. These large animal data support the concept that, with further development, gene editing approaches may prove clinically useful for the treatment of DMD.

The persistent contraction and relaxation of cardiac and skeletal muscles necessitates mechanisms that maintain the integrity of muscle membranes (*1*, *2*). Dystrophin is a large scaffolding protein that supports muscle structure and function by linking the cytoskeleton with the sarcolemma of muscle tissue (*1*, *3*, *4*). Mutations in the dystrophin gene cause Duchenne muscular dystrophy (DMD), a disorder primarily affecting boys that is characterized by progressive muscle degeneration and atrophy, leading to premature death from cardiomyopathy and respiratory collapse (*5*). Thousands of mutations have been identified in the dystrophin gene, which spans ~2.5 megabases of DNA and contains 79 exons. Many of these mutations cluster into "hot spots", most commonly in a region that spans exons 45 to 50, typically placing exon 51 out of frame with preceding exons and preventing expression of functional dystrophin protein (*6*, *7*). Therapies that induce "skipping" of exon 51 restore the reading frame, and in principle could benefit approximately 13% of DMD patients (*8*). An oligonucleotide that allows skipping of exon 51 can restore dystrophin expression to 0.22 to 0.32% of normal levels after one year of treatment and has been approved for DMD patients (*9*–*13*).

CRISPR/Cas9 gene editing can target DMD mutations and restore dystrophin expression in mice and muscle cells derived from human induced pluripotent stem cells (iPSCs) (*14*–*22*). An essential step toward clinical translation of gene editing as a therapeutic strategy for DMD is the demonstration of efficacy and safety of this approach in large mammals.

The mutation carried by the deltaE50-MD canine model of DMD leads to loss of exon 50 and moreover can be corrected by skipping of exon 51, making this a valuable model for translational studies. First identified as a naturally occurring, spontaneous mutation in Cavalier King Charles Spaniels (*23*) and now maintained on a beagle background, this model (in contrast to mice) exhibits many of the clinical and pathological features of the human disease, such as muscle weakness, atrophy and fibrosis (*24*).

To correct the dystrophin reading frame in the deltaE50-MD canine model (henceforth referred to as ΔEx50) (Fig. 1A), we used *S. pyogenes* Cas9 coupled with a sgRNA to target a region adjacent to the exon 51 splice acceptor site (referred to as sgRNA-51) (Fig. 1B). The sgRNA-51 corresponded to a highly conserved sequence that differs by only one nucleotide between the human and dog genomes (fig. S1A). Cas9 coupled with each of these sgRNA-51 sequences introduced a genomic cut only in DNA of the respective species (fig. S1B).

For the in vivo delivery of Cas9 and sgRNA-51 to skeletal muscle and heart tissue in dogs, we used recombinant adeno-associated virus serotype 9 (referred to as AAV9), which displays preferential tropism for these tissues (*25*, *26*). A muscle-specific creatine kinase (CK) regulatory cassette was used to drive expression of Cas9; three RNA polymerase III

promoters (U6, H1 and 7SK) directed expression of the sgRNA, as described previously in mice (fig. S2) (*18*). AAV9-Cas9 and AAV9-sgRNA-51 were initially introduced into the cranial tibialis muscles of two 1 month-old dogs by intra-muscular (IM) injection with $1.2x10^{13}$ AAV9 viral genomes (vg) of each virus. Muscles were analyzed 6 weeks after injection. In vivo targeting efficiency was estimated within muscle biopsy samples by RT-PCR with primers for sequences in exons 48 and 53, and genomic PCR amplification products spanning the target site were subjected to amplicon deep-sequencing. The latter indicated that a mean of 9.96% of total reads contained changes at the targeted genomic site including insertions, deletions and substitutions (fig. S3). The most commonly identified mutations with a mean of 2.35% contained an adenosine (A) insertion immediately 3' to the Cas9 genomic cutting site (Fig. 1C). The deletions identified using this method encompassed a highly-predicted exonic splicing enhancer (ESE) site for exon 51 (*18*, *27*, *28*) (fig. S3A). However, this method does not identify larger deletions that might occur beyond the annealing sites of the primers used for PCR. Since these tissue samples contain a mixture of muscle and non-muscle cells, the method likely underestimates the efficiency of gene editing within muscle cells.

Sequencing of RT-PCR products of RNA from muscle of ΔEx50 dogs injected intramuscularly with AAV9-Cas9 and AAV9-sgRNA-51 showed that deletion of exon 51 (ΔEx50-51) allowed splicing from exon 49 to 52, which restores the dystrophin open reading frame (fig. S3B). On gels, the PCR product with the A insertion was indistinguishable in size from non-edited cDNA products, so we performed deep-sequencing analysis to quantify its abundance compared to other small insertions. Deep-sequencing of the upper band containing the non-edited cDNA product and reframed cDNA products indicated that a mean of 73.19% of total reads contained reframed cDNA products with an A insertion, a mean of 26.81% contained non-edited cDNA product, and the rest contained small deletions and insertions (fig. S3C). However, nonsense mediated decay might impact the abundance of non-edited cDNA produtcs. These data indicate that the two ΔEx50 dogs injected with AAV9-Cas9 and AAV9-sgRNA-51 had a high frequency of reframing events (with cDNA products containing an A insertion in the sequence of exon 51) and exon 51 skipping events resulting from deletion of the highly conserved ESE region.

To evaluate the specificity of our gene editing approach, we analyzed predicted off-target genomic sites for possible promiscuous editing. A total of three potential genome-wide off-target sites (OT1 to OT3) (fig. S4) were predicted in coding exons and 4 in non-coding regions (fig. S4) by the CRISPR design tool (http://crispr.mit.edu/). We performed deep sequencing at the top predicted off-target sites within protein-coding exons. None of these sites revealed significantly more sequence alterations than the background analysis performed with other regions of the amplicons (fig. S5).

To evaluate dystrophin correction at the protein level, we performed histological analysis of AAV9-injected cranial tibialis muscles 6 weeks after AAV9 injection. Dystrophin immunohistochemistry of muscle from ΔEx50 dogs injected with AAV9-Cas9 and AAV-sgRNA-51 revealed widespread expression: the majority of fibers within the injected muscles expressed sarcolemmal dystrophin, albeit to varying levels (Fig. 1D). Western blot analysis confirmed the restoration of dystrophin expression in skeletal muscle (Fig. 2, A and B) to ~60% of wild-type levels. On average, 2% of wild-type levels of dystrophin were detected in the uninjected contralateral muscles, far more than could be attributed to rare revertant events, which typically represent fewer than 0.001% of fibers and are undetectable by Western blot in ΔEx50 muscle. We attribute expression in uninjected contralateral muscles to leakage of AAV9 into circulation. As assessed by H&E staining, the injected muscles appeared to be normalized relative to muscles of untreated animals, with fewer hypercontracted or necrotic fibers, reduced edema and fibrosis, and fewer regions of inflammatory cellular infiltration (Fig. 2C). Immunohistochemistry for developmental myosin heavy chain (dMHC), a marker of regenerating fibers, revealed a marked reduction in developmental myosin (dMHC)-positive fibers within injected muscles (fig. S6).

Dystrophin nucleates a series of proteins into the dystrophin-associated glycoprotein complex (DGC) to link the cytoskeleton and extracellular matrix (*3*, *4*). In ΔEx50 mice, dogs, and DMD patients, these proteins are destabilized and do not localize to the sub-sarcolemmal region (*4*). Muscles injected with AAV9-Cas9 and AAV9-sgRNA-51 showed recovery of the DGC protein beta-dystroglycan compared to contralateral uninjected muscles (fig. S7). We conclude that – at least in a short time frame of 6 weeks–single-cut genomic editing using AAV9-Cas9 and AAV9-sgRNA-51 can efficiently restore dystrophin expression and assembly of the DGC in dystrophic muscles. Immunohistochemistry using canine-specific CD4 and CD8 T cell markers (fig. S8), showed no evidence of enhanced mononuclear cellular infiltration or relevant hematological abnormalities in the treated animals compared to untreated controls or reference ranges (fig. S9).

Based on the high dystrophin-correction efficiency observed following IM injection of AAV9-Cas9 and AAV9-sgRNA-51, we tested for rescue of dystrophin expression in two ΔEx50 dogs after systemic delivery of gene editing components. The dogs at 1 month of age were injected intravenously with the viruses and analyzed 8 weeks later. We tested two doses ($2x10^{13}$ vg/kg and $1x10^{14}$ vg/kg) of each of the two viruses (AAV9-Cas9 and AAV9-sgRNA-51). To avoid a possible immune reaction, we included a transient regimen of immune suppression with the high dose. Systemic delivery of

$2x10^{13}$ vg/kg of each virus (total virus $4x10^{13}$ vg/kg) in ΔEx50-Dog-#2A resulted in expression of virus in peripheral skeletal muscle samples, and to a lower extent in heart samples, as shown by qPCR analysis (fig. S10A). The delivery of $1x10^{14}$ vg/kg of each virus (total virus $2x10^{14}$ vg/kg) in ΔEx50-Dog-#2B (via infusion) allowed more widespread expression of viral constructs in the peripheral skeletal muscle samples and in heart samples (fig. S10B). Systemic delivery of AAV9-Cas9 and AAV9-sgRNA-51 led to dystrophin expression in a broad range of muscles, including the heart, in gene-edited ΔEx50 dogs at 8 weeks post-injection, and to a markedly greater extent than that achieved with the lower dose (Fig. 3).

To investigate the proportions of various indels generated by systemic delivery of AAV9-Cas9 and AAV9-sgRNA-51, we performed amplicon deep-sequencing analysis of the genomic DNA from heart, triceps and biceps muscles. The genomic deep-sequencing analysis revealed an increase of percentage of reads containing changes at the targeted genomic site, especially of the 1A insertion mutation in the samples from Dog-#2B compared to Dog-#2A (fig. S11).

Additionally, we performed tracking indels by decomposition (TIDE) (*30*) analysis at the genomic and cDNA levels, which showed an increase in numbers of indels in the samples from Dog-#2B compared to the samples from Dog-#2A (fig. S12). Testes analysis and Western blot analysis showed no activity of Cas9 and confirmed muscle specific expression of gene editing machinery (fig. S13). Western blot analysis confirmed the restoration of dystrophin expression in skeletal muscle (Fig. 4, A and B) to levels ~50%, 20% and 3% of wild-type levels for the cranial tibialis, triceps, and biceps, respectively, after systemic delivery of $2x10^{13}$ vg/kg of each virus (total virus $4x10^{13}$ vg/kg). For Dog-#2B, which received $1x10^{14}$ vg/kg of each virus (total virus $2x10^{14}$ vg/kg), Western blot analysis showed restoration of dystrophin expression (Fig. 4, C, D and fig. S14) to levels ~70%, 25%, 64%, 58%, 92% and 5% of wild-type levels for the cranial tibialis, triceps, biceps, diaphragm, heart and tongue muscles, respectively. Similar to what was seen after IM injection, muscles appeared normalized via H&E staining (Fig. 4E). Immunostaining of muscle sections from treated ΔEx50 dogs also showed recovery of beta-dystroglycan expression (fig. S15) and widespread reduction in dMHC, a marker of muscle regeneration (fig. S16).

To determine hematological and biochemical parameters of the treated dogs compared to the controls, we collected blood samples the day before injection and then at 1, 2, 4, 6 and 8 weeks post-injection. The blood samples from all 4 dogs (healthy untreated, ΔEx50 untreated, and ΔEx50 dogs receiving $2x10^{13}$ vg/kg of each virus (total virus $4x10^{13}$ vg/kg) and $1x10^{14}$ vg/kg of each virus (total virus $2x10^{14}$ vg/kg) before and after injection were unremarkable (fig. S17). Hematology counts, serum electrolytes and kidney/liver function parameters remained within the normal ranges in all dogs. Additionally, blood samples were collected weekly for CK assessment: we observed a modest decline in serum CK activity in Dog-#2B treated with $1x10^{14}$ vg/kg of each virus (total virus $2x10^{14}$ vg/kg) (fig. S18) compared to ΔEx50 untreated dog.

To evaluate the targeting efficiency of a human DMD mutation, we used a DMD iPSC line carrying a deletion from exon 48 to 50. Deletion of exons 48 to 50 leads to a frameshift mutation and appearance of a premature stop codon in exon 51. To correct the dystrophin reading frame, we introduced two concentrations of Cas9 and sgRNA-51 (26ng/μl, referred to as high, and 13ng/μl, referred to as low). Indel analysis showed 55.8% and 31.9% of indels for the high and low concentrations, respectively (fig. S19). Genomic deep-sequencing analysis revealed that 27.94% of mutations contained a single A insertion 3' to the PAM sequence for the high concentration condition and 19.03% for the low concentration condition (fig. S20A), as observed in mouse and dog cells with a similar sgRNA directed against same genomic locus. DMD iPSCs treated with Cas9 and sgRNA-51 and induced to form cardiomyocytes (iCMs) showed restoration of dystrophin immunostaining (fig. S20B) and expression of dystrophin protein to levels that were 67 - 100% of the levels of WT cardiomyocytes, as measured by Western blot (fig. S20C and D).

It has been estimated that even 15% of normal levels of dystrophin would provide significant therapeutic benefits for DMD patients (*30–32*). Our results demonstrate the efficacy of single cut genome editing for restoration of dystrophin expression in a large animal model of DMD, reaching up to ~80% of wild-type levels in some muscles after 8 weeks. Longer-term studies are required to establish whether the expression of dystrophin and the maintenance of muscle integrity we observed are sustained.

This study, while encouraging, is preliminary and has several limitations, including the relatively small number of animals analyzed and the short duration of the analysis (6-8 weeks). The possibility of off-target effects of in vivo gene editing is a further potential safety concern. While our initial deep sequencing analysis of the top predicted off-target sites revealed no specific off-target gene editing above background levels in treated animals, it will be important to further assess possible off-target mutagenesis in longer term studies with greater numbers of animals. Recent studies reported large deletions and complex genomic rearrangements at target sites of CRISPR-Cas9 in mouse embryonic cells, hematopoietic progenitors and human immortalized epithelial cells (*33*). However, these cells are highly proliferative, more genomically unstable in culture and use different DNA repair pathways than somatic post-mitotic cells (such as muscle and heart cells) (*34*). Future studies will be required to investigate the long-term genomic stability of gene-edited muscle tissues in vivo. Another potential concern with CRISPR/Cas9-mediated gene editing in vivo is immunogenicity of Cas9,

particularly as expression persists post initial treatment. In this short-term study, we did not observe CD4- or CD8-positive cell infiltration of treated muscle, but longer-term studies with more sensitive assays must be performed. Additionally, although production of large quantities of AAV9 poses a challenge, doses of $2x10^{14}$vg/kg have been successfully used in human gene therapy trials (*35*).

Finally, although gene editing and exon skipping oligos can both restore production of internally deleted dystrophin proteins, similar to those expressed in Becker muscular dystrophy, there are key distinctions between these approaches. Most notably, CRISPR gene editing may be permanent and not require re-delivery whereas oligos require continuous treatment. A corollary of this is that CRISPR treatment may be difficult to terminate if safety concerns arise.

REFERENCES AND NOTES

1. K. F. O'Brien, L. M. Kunkel, Dystrophin and muscular dystrophy: Past, present, and future. *Mol. Genet. Metab.* **74**, 75–88 (2001). doi:10.1006/mgme.2001.3220 Medline
2. S. Guiraud, A. Aartsma-Rus, N. M. Vieira, K. E. Davies, G.-J. B. van Ommen, L. M. Kunkel, The Pathogenesis and Therapy of Muscular Dystrophies. *Annu. Rev. Genomics Hum. Genet.* **16**, 281–308 (2015). doi:10.1146/annurev-genom-090314-025003 Medline
3. K. P. Campbell, S. D. Kahl, Association of dystrophin and an integral membrane glycoprotein. *Nature* **338**, 259–262 (1989). doi:10.1038/338259a0 Medline
4. J. M. Ervasti, K. Ohlendieck, S. D. Kahl, M. G. Gaver, K. P. Campbell, Deficiency of a glycoprotein component of the dystrophin complex in dystrophic muscle. *Nature* **345**, 315–319 (1990). doi:10.1038/345315a0 Medline
5. F. Muntoni, S. Torelli, A. Ferlini, Dystrophin and mutations: One gene, several proteins, multiple phenotypes. *Lancet Neurol.* **2**, 731–740 (2003). doi:10.1016/S1474-4422(03)00585-4 Medline
6. C. L. Bladen, D. Salgado, S. Monges, M. E. Foncuberta, K. Kekou, K. Kosma, H. Dawkins, L. Lamont, A. J. Roy, T. Chamova, V. Guergueltcheva, S. Chan, L. Korngut, C. Campbell, Y. Dai, J. Wang, N. Barišić, P. Brabec, J. Lahdetie, M. C. Walter, O. Schreiber-Katz, V. Karcagi, M. Garami, V. Viswanathan, F. Bayat, F. Buccella, E. Kimura, Z. Koeks, J. C. van den Bergen, M. Rodrigues, R. Roxburgh, A. Lusakowska, A. Kostera-Pruszczyk, J. Zimowski, R. Santos, E. Neagu, S. Artemieva, V. M. Rasic, D. Vojinovic, M. Posada, C. Bloetzer, P.-Y. Jeannet, F. Joncourt, J. Díaz-Manera, E. Gallardo, A. A. Karaduman, H. Topaloğlu, R. El Sherif, A. Stringer, A. V. Shatillo, A. S. Martin, H. L. Peay, M. I. Bellgard, J. Kirschner, K. M. Flanigan, V. Straub, K. Bushby, J. Verschuuren, A. Aartsma-Rus, C. Béroud, H. Lochmüller, The TREAT-NMD DMD Global Database: Analysis of more than 7,000 Duchenne muscular dystrophy mutations. *Hum. Mutat.* **36**, 395–402 (2015). doi:10.1002/humu.22758 Medline
7. Y. Li, Z. Liu, S. OuYang, Y. Zhu, L. Wang, J. Wu, Distribution of dystrophin gene deletions in a Chinese population. *J. Int. Med. Res.* **44**, 99–108 (2016). doi:10.1177/0300060515613223 Medline
8. A. Aartsma-Rus, I. Fokkema, J. Verschuuren, I. Ginjaar, J. van Deutekom, G.-J. van Ommen, J. T. den Dunnen, Theoretic applicability of antisense-mediated exon skipping for Duchenne muscular dystrophy mutations. *Hum. Mutat.* **30**, 293–299 (2009). doi:10.1002/humu.20918 Medline
9. Y. Shimizu-Motohashi, S. Miyatake, H. Komaki, S. Takeda, Y. Aoki, Recent advances in innovative therapeutic approaches for Duchenne muscular dystrophy: From discovery to clinical trials. *Am. J. Transl. Res.* **8**, 2471–2489 (2016). Medline
10. C. A. Stein, Eteplirsen Approved for Duchenne Muscular Dystrophy: The FDA Faces a Difficult Choice. *Mol. Ther.* **24**, 1884–1885 (2016). doi:10.1038/mt.2016.188 Medline
11. A. Aartsma-Rus, A. M. Krieg, FDA Approves Eteplirsen for Duchenne Muscular Dystrophy: The Next Chapter in the Eteplirsen Saga. *Nucleic Acid Ther.* **27**, 1–3 (2017). doi:10.1089/nat.2016.0657 Medline
12. J. J. Dowling, Eteplirsen therapy for Duchenne muscular dystrophy: Skipping to the front of the line. *Nat. Rev. Neurol.* **12**, 675–676 (2016). doi:10.1038/nrneurol.2016.180 Medline
13. J. R. Mendell, N. Goemans, L. P. Lowes, L. N. Alfano, K. Berry, J. Shao, E. M. Kaye, E. Mercuri; Eteplirsen Study Group and Telethon Foundation DMD Italian Network, Longitudinal effect of eteplirsen versus historical control on ambulation in Duchenne muscular dystrophy. *Ann. Neurol.* **79**, 257–271 (2016). doi:10.1002/ana.24555 Medline
14. C. Long, L. Amoasii, A. A. Mireault, J. R. McAnally, H. Li, E. Sanchez-Ortiz, S. Bhattacharyya, J. M. Shelton, R. Bassel-Duby, E. N. Olson, Postnatal genome editing partially restores dystrophin expression in a mouse model of muscular dystrophy. *Science* **351**, 400–403 (2016). doi:10.1126/science.aad5725 Medline
15. M. Tabebordbar, K. Zhu, J. K. W. Cheng, W. L. Chew, J. J. Widrick, W. X. Yan, C. Maesner, E. Y. Wu, R. Xiao, F. A. Ran, L. Cong, F. Zhang, L. H. Vandenberghe, G. M. Church, A. J. Wagers, In vivo gene editing in dystrophic mouse muscle and muscle stem cells. *Science* **351**, 407–411 (2016). doi:10.1126/science.aad5177 Medline
16. C. E. Nelson, C. H. Hakim, D. G. Ousterout, P. I. Thakore, E. A. Moreb, R. M. Castellanos Rivera, S. Madhavan, X. Pan, F. A. Ran, W. X. Yan, A. Asokan, F. Zhang, D. Duan, C. A. Gersbach, In vivo genome editing improves muscle function in a mouse model of Duchenne muscular dystrophy. *Science* **351**, 403–407 (2016). doi:10.1126/science.aad5143 Medline
17. C. Long, H. Li, M. Tiburcy, C. Rodriguez-Caycedo, V. Kyrychenko, H. Zhou, Y. Zhang, Y.-L. Min, J. M. Shelton, P. P. A. Mammen, N. Y. Liaw, W.-H. Zimmermann, R. Bassel-Duby, J. W. Schneider, E. N. Olson, Correction of diverse muscular dystrophy mutations in human engineered heart muscle by single-site genome editing. *Sci. Adv.* **4**, p9004 (2018). doi:10.1126/sciadv.aap9004 Medline
18. L. Amoasii, C. Long, H. Li, A. A. Mireault, J. M. Shelton, E. Sanchez-Ortiz, J. R. McAnally, S. Bhattacharyya, F. Schmidt, D. Grimm, S. D. Hauschka, R. Bassel-Duby, E. N. Olson, Single-cut genome editing restores dystrophin expression in a new mouse model of muscular dystrophy. *Sci. Transl. Med.* **9**, eaan8081 (2017). doi:10.1126/scitranslmed.aan8081 Medline
19. N. E. Bengtsson, J. K. Hall, G. L. Odom, M. P. Phelps, C. R. Andrus, R. D. Hawkins, S. D. Hauschka, J. R. Chamberlain, J. S. Chamberlain, Muscle-specific CRISPR/Cas9 dystrophin gene editing ameliorates pathophysiology in a mouse model for Duchenne muscular dystrophy. *Nat. Commun.* **8**, 14454 (2017). doi:10.1038/ncomms14454 Medline
20. J. P. Tremblay, J.-P. Iyombe-Engembe, B. Duchêne, D. L. Ouellet, Gene Editing for Duchenne Muscular Dystrophy Using the CRISPR/Cas9 Technology: The Importance of Fine-tuning the Approach. *Mol. Ther.* **24**, 1888–1889 (2016). doi:10.1038/mt.2016.191 Medline
21. C. S. Young, M. R. Hicks, N. V. Ermolova, H. Nakano, M. Jan, S. Younesi, S. Karumbayaram, C. Kumagai-Cresse, D. Wang, J. A. Zack, D. B. Kohn, A. Nakano, S. F. Nelson, M. C. Miceli, M. J. Spencer, A. D. Pyle, A single CRISPR-Cas9 deletion strategy that targets the majority of DMD patients restores dystrophin function in hiPSC-derived muscle cells. *Cell Stem Cell* **18**, 533–540 (2016). Medline
22. D. G. Ousterout, A. M. Kabadi, P. I. Thakore, W. H. Majoros, T. E. Reddy, C. A. Gersbach, Multiplex CRISPR/Cas9-based genome editing for correction of dystrophin mutations that cause Duchenne muscular dystrophy. *Nat. Commun.* **6**, 6244 (2015). doi:10.1038/ncomms7244 Medline
23. G. L. Walmsley, V. Arechavala-Gomeza, M. Fernandez-Fuente, M. M. Burke, N. Nagel, A. Holder, R. Stanley, K. Chandler, S. L. Marks, F. Muntoni, G. D. Shelton, R. J. Piercy, A duchenne muscular dystrophy gene hot spot mutation in dystrophin-deficient cavalier king charles spaniels is amenable to exon 51 skipping. *PLOS ONE* **5**, e8647 (2010). doi:10.1371/journal.pone.0008647 Medline
24. J. Hildyard, F. Rawson, R. Harron, D. Riddell, C. Massey, F. Taylor-Brown, D. J. Wells, R. J. Piercy, Characterising the skeletal muscle histological phenotype of the DeltaE50-MD dog, a preclinical model of Duchenne muscular dystrophy. *Neuromuscul. Disord.* **28**, S18 (2018). doi:10.1016/S0960-8966(18)30342-0
25. Y. Yue, X. Pan, C. H. Hakim, K. Kodippili, K. Zhang, J.-H. Shin, H. T. Yang, T. McDonald, D. Duan, Safe and bodywide muscle transduction in young adult Duchenne muscular dystrophy dogs with adeno-associated virus. *Hum. Mol. Genet.* **24**, 5880–5890 (2015). doi:10.1093/hmg/ddv310 Medline
26. C. Zincarelli, S. Soltys, G. Rengo, J. E. Rabinowitz, Analysis of AAV serotypes 1-9 mediated gene expression and tropism in mice after systemic injection. *Mol. Ther.* **16**, 1073–1080 (2008). doi:10.1038/mt.2008.76 Medline
27. P. J. Smith, C. Zhang, J. Wang, S. L. Chew, M. Q. Zhang, A. R. Krainer, An increased

specificity score matrix for the prediction of SF2/ASF-specific exonic splicing enhancers. *Hum. Mol. Genet.* **15**, 2490–2508 (2006). doi:10.1093/hmg/ddl171 Medline
28. L. Cartegni, J. Wang, Z. Zhu, M. Q. Zhang, A. R. Krainer, ESEfinder: A web resource to identify exonic splicing enhancers. *Nucleic Acids Res.* **31**, 3568–3571 (2003). doi:10.1093/nar/gkg616 Medline
29. E. K. Brinkman, T. Chen, M. Amendola, B. van Steensel, Easy quantitative assessment of genome editing by sequence trace decomposition. *Nucleic Acids Res.* **42**, e168 (2014). doi:10.1093/nar/gku936 Medline
30. C. Godfrey, S. Muses, G. McClorey, K. E. Wells, T. Coursindel, R. L. Terry, C. Betts, S. Hammond, L. O'Donovan, J. Hildyard, S. El Andaloussi, M. J. Gait, M. J. Wood, D. J. Wells, How much dystrophin is enough: The physiological consequences of different levels of dystrophin in the mdx mouse. *Hum. Mol. Genet.* **24**, 4225–4237 (2015). doi:10.1093/hmg/ddv155 Medline
31. M. van Putten, E. M. van der Pijl, M. Hulsker, I. E. C. Verhaart, V. D. Nadarajah, L. van der Weerd, A. Aartsma-Rus, Low dystrophin levels in heart can delay heart failure in mdx mice. *J. Mol. Cell. Cardiol.* **69**, 17–23 (2014). doi:10.1016/j.yjmcc.2014.01.009 Medline
32. A. H. Beggs, E. P. Hoffman, J. R. Snyder, K. Arahata, L. Specht, F. Shapiro, C. Angelini, H. Sugita, L. M. Kunkel, Exploring the molecular basis for variability among patients with Becker muscular dystrophy: Dystrophin gene and protein studies. *Am. J. Hum. Genet.* **49**, 54–67 (1991). Medline
33. M. Kosicki, K. Tomberg, A. Bradley, Repair of double-strand breaks induced by CRISPR-Cas9 leads to large deletions and complex rearrangements. *Nat. Biotechnol.* **36**, 765–771 (2018). Medline
34. E. D. Tichy, R. Pillai, L. Deng, L. Liang, J. Tischfield, S. J. Schwemberger, G. F. Babcock, P. J. Stambrook, Mouse embryonic stem cells, but not somatic cells, predominantly use homologous recombination to repair double-strand DNA breaks. *Stem Cells Dev.* **19**, 1699–1711 (2010). doi:10.1089/scd.2010.0058 Medline
35. J. R. Mendell, S. Al-Zaidy, R. Shell, W. D. Arnold, L. R. Rodino-Klapac, T. W. Prior, L. Lowes, L. Alfano, K. Berry, K. Church, J. T. Kissel, S. Nagendran, J. L'Italien, D. M. Sproule, C. Wells, J. A. Cardenas, M. D. Heitzer, A. Kaspar, S. Corcoran, L. Braun, S. Likhite, C. Miranda, K. Meyer, K. D. Foust, A. H. M. Burghes, B. K. Kaspar, Single-Dose Gene-Replacement Therapy for Spinal Muscular Atrophy. *N. Engl. J. Med.* **377**, 1713–1722 (2017). doi:10.1056/NEJMoa1706198 Medline

ACKNOWLEDGMENTS

We thank V. Malladi (UT Southwestern Department of Clinical Sciences) for bioinformatics analysis, D. Church, S. Niessen and D. Wells (RVC) for helpful research and clinical advice, staff and veterinarians within the RVC Biological Sciences Unit for technical assistance and animal care, C. Rodriguez for assistance and J. Cabrera for graphics. We are grateful to S. Hauschka (University of Washington) for the CK8 promoter. **Funding:** This work was supported by grants from the NIH (HL130253, HL-077439, DK-099653, and AR-067294), Senator Paul D. Wellstone Muscular Dystrophy Cooperative Research Center grant (U54 HD 087351), the Robert A. Welch Foundation (grant 1-0025 to E.N.O.) and Exonics Therapeutics. The RVC dog colony program was established and/or is supported by grants from the Wellcome Trust (101550/Z/13/Z) Muscular Dystrophy UK (RA3/3077) and from Duchenne Ireland. **Author contributions:** L.A., J.C.W.H., C.M., T.S., R.H. and R.P performed the animal procedures; L.A., J.H., H.L., J.M.S., E. S.-O. performed the experiments; A.M. and D.C performed tissues pulverization; R. H and C.M assisted for the animal care and procedure. **Competing interests:** L.A., R.B.D, R.P. and E.N.O. are consultants for Exonics Therapeutics. L.A. and E.N.O. are co-inventors on a patent application (provisional filing number 62/442,606) related to the strategy presented in this study. The other authors declare no competing interests. **Data and materials availability:** All data needed to evaluate the conclusions in the paper are present in the paper.

SUPPLEMENTARY MATERIALS

www.sciencemag.org/cgi/content/full/science.aau1549/DC1
Materials and Methods
Figs. S1 to S20
Table S1

11 May 2018; accepted 17 August 2018
Published online 30 August 2018
10.1126/science.aau1549

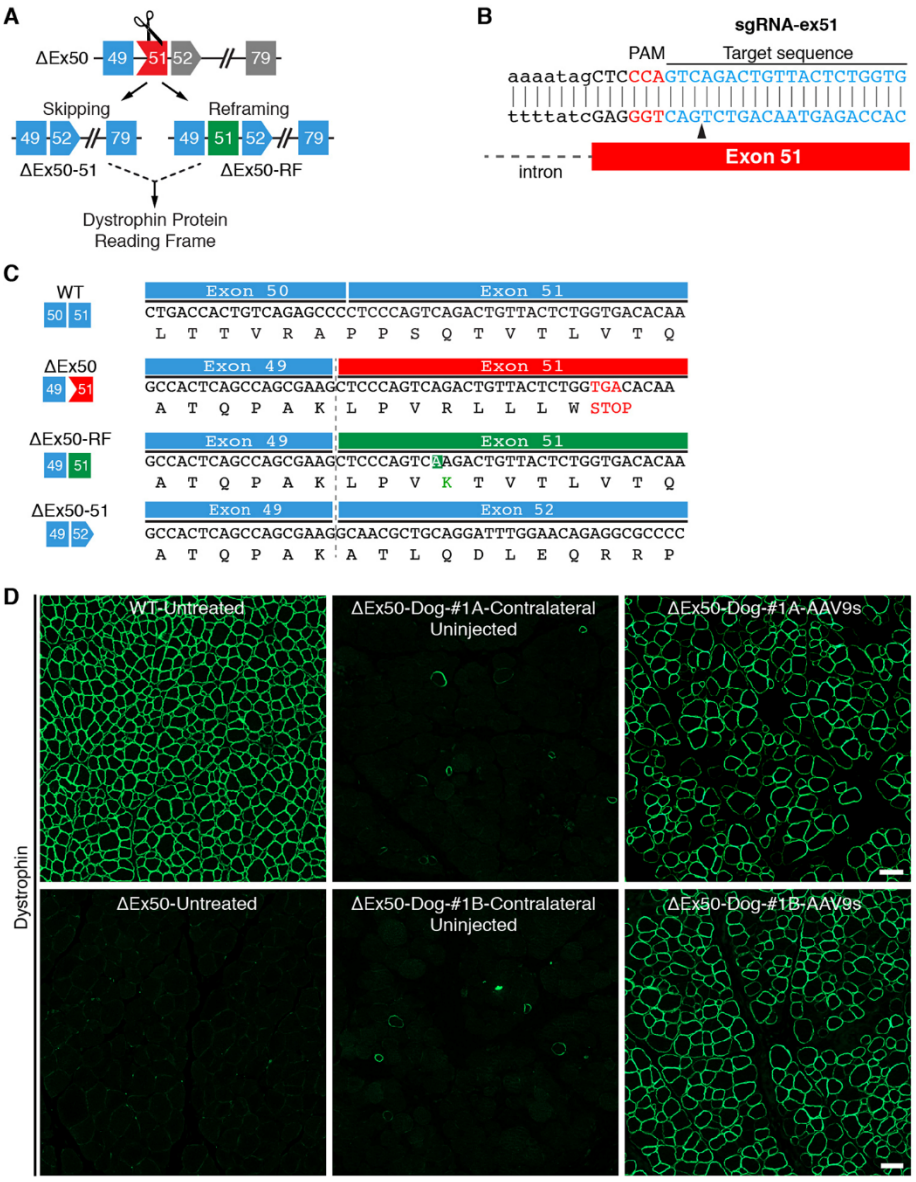

Fig. 1. Fig. 1. Single cut CRISPR editing of canine exon 50 in vivo and in vitro. (**A**) Scheme showing the CRISPR/Cas9-mediated genome editing approach to correct the reading frame in ΔEx50 dogs by reframing and skipping of exon 51. Gray exons are out of frame. (**B**) Illustration of sgRNA binding position and sequence for sgRNA-ex51. PAM sequence for sgRNA is indicated in red. Black arrow indicates the cleavage site. (**C**) Sequence of the RT-PCR products of the ΔEx50-51 lower band confirmed that exon 49 spliced directly to exon 52, excluding exon 51. Sequence of RT-PCR products of ΔEx50 reframed (ΔEx50-RF). (**D**) Cranial tibialis muscles of ΔEx50 dogs were injected with AAV9s encoding sgRNA-51 and Cas9 as schematized in Fig. 1 and analyzed 6 weeks later. Dystrophin immunohistochemistry staining of cranial tibialis muscle of wild type dog untreated, ΔEx50 dog untreated, ΔEx50 dogs contralateral (uninjected) muscle and ΔEx50 dogs injected with AAV9-Cas9 and AAV9-sgRNA-51 (referred as ΔEx50-#1A-AAV9s and ΔEx50-#1B-AAV9s). Scale bar: 50μm.

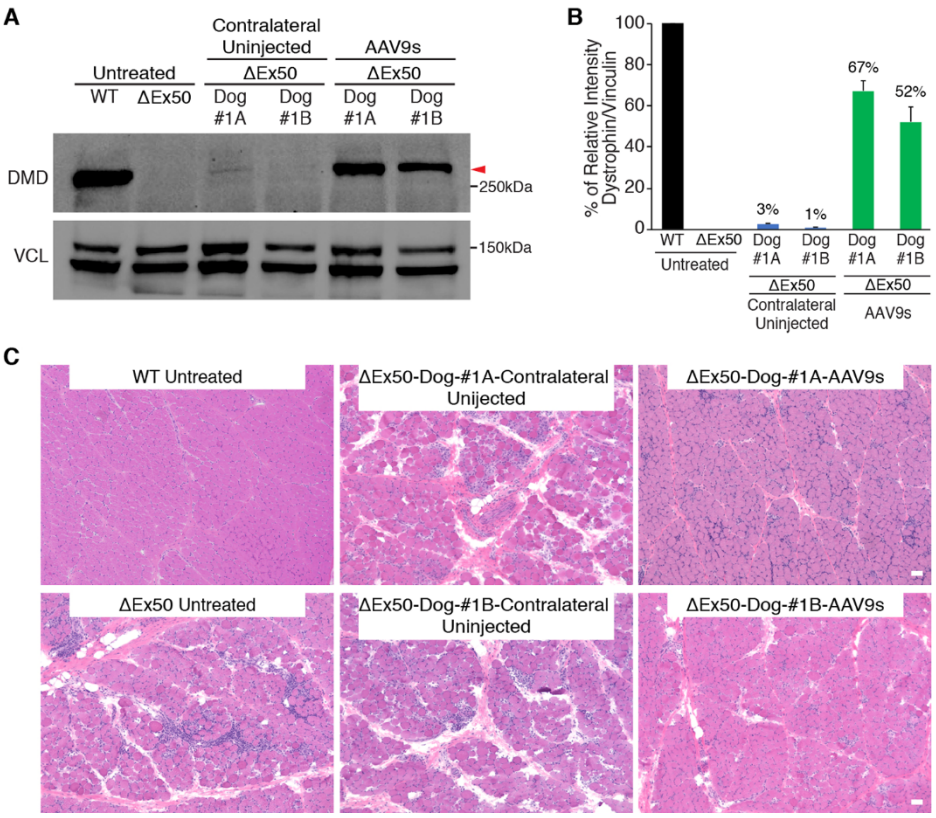

Fig. 2. Dystrophin correction following intramuscular delivery of AAV9-encoded gene editing components. (**A**) Western blot analysis of dystrophin (DMD) and vinculin (VCL) expression in cranial tibialis muscles 6 weeks after intramuscular injection in 2 dogs (#1A and #1B). (**B**) Quantification of dystrophin expression from blots after normalization to vinculin. (**C**) Histochemistry by hematoxylin and eosin (H&E) staining of cranial tibialis muscle from a wild type dog, ΔEx50 dog untreated, ΔEx50 contralateral uninjected and ΔEx50 dogs injected intramuscularly with AAV9-Cas9 and AAV9-sgRNA-51 (referred as ΔEx50-Dog-#1A-AAV9s and ΔEx50-Dog-#1B-AAV9s). Scale bar: 50μm.

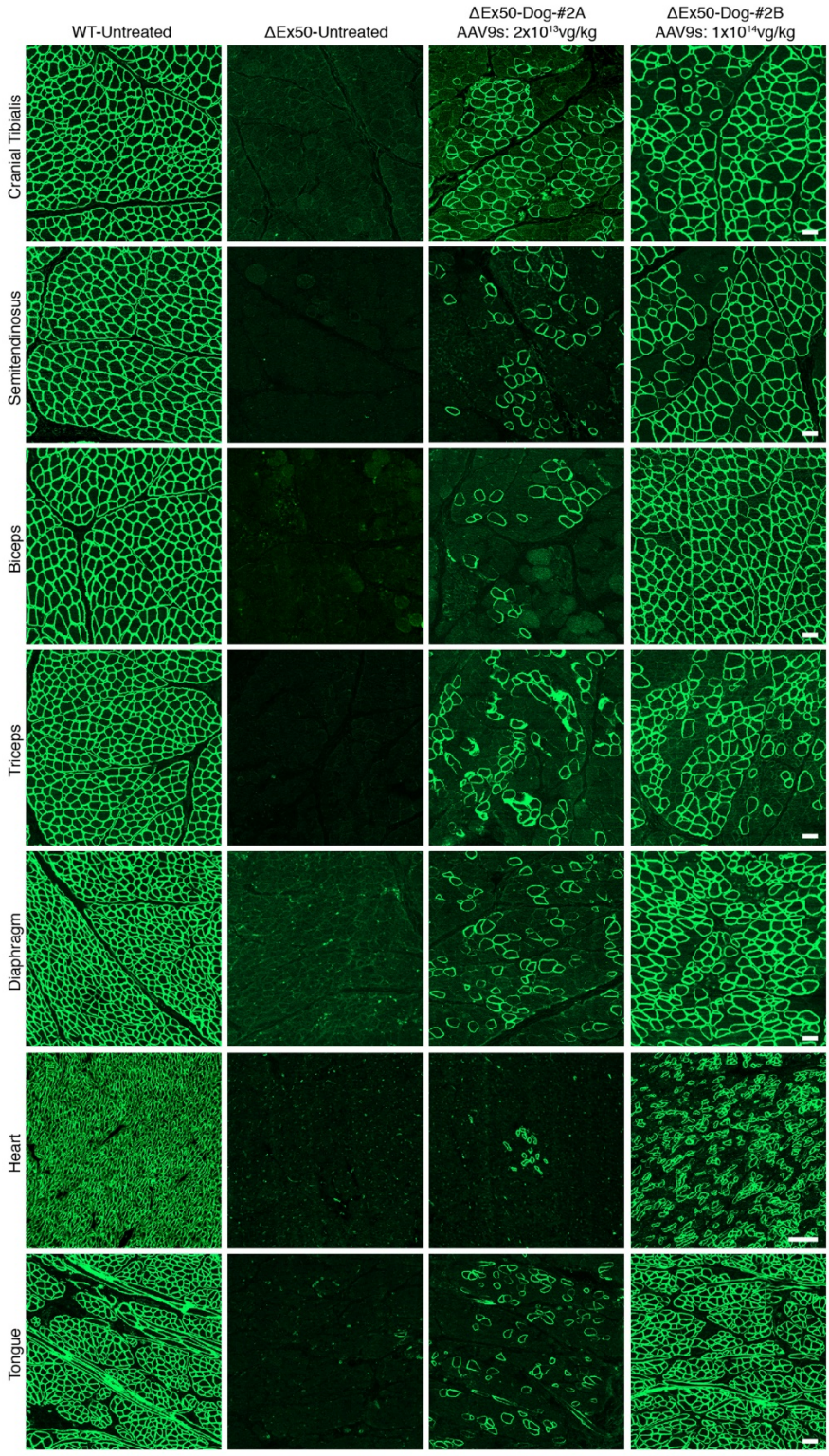

Fig. 3. Immunostaining of dystrophin following intravenous delivery of AAV9-encoded gene editing components. Dystrophin immunohistochemistry staining of cranial tibialis, semitendinosus, biceps, triceps, diaphragm, heart and tongue muscles of wild type dog, untreated ΔEx50 dog, and ΔEx50 dogs injected systemically with AAV9-Cas9 and AAV9-sgRNA at $2x10^{13}$vg/kg (total virus $4x10^{13}$ vg/kg, referred as ΔEx50-Dog #2A-AAV9s) and $1x10^{14}$ vg/kg (total virus $2x10^{14}$ vg/kg, referred as ΔEx50-Dog #2B-AAV9s) for each virus.

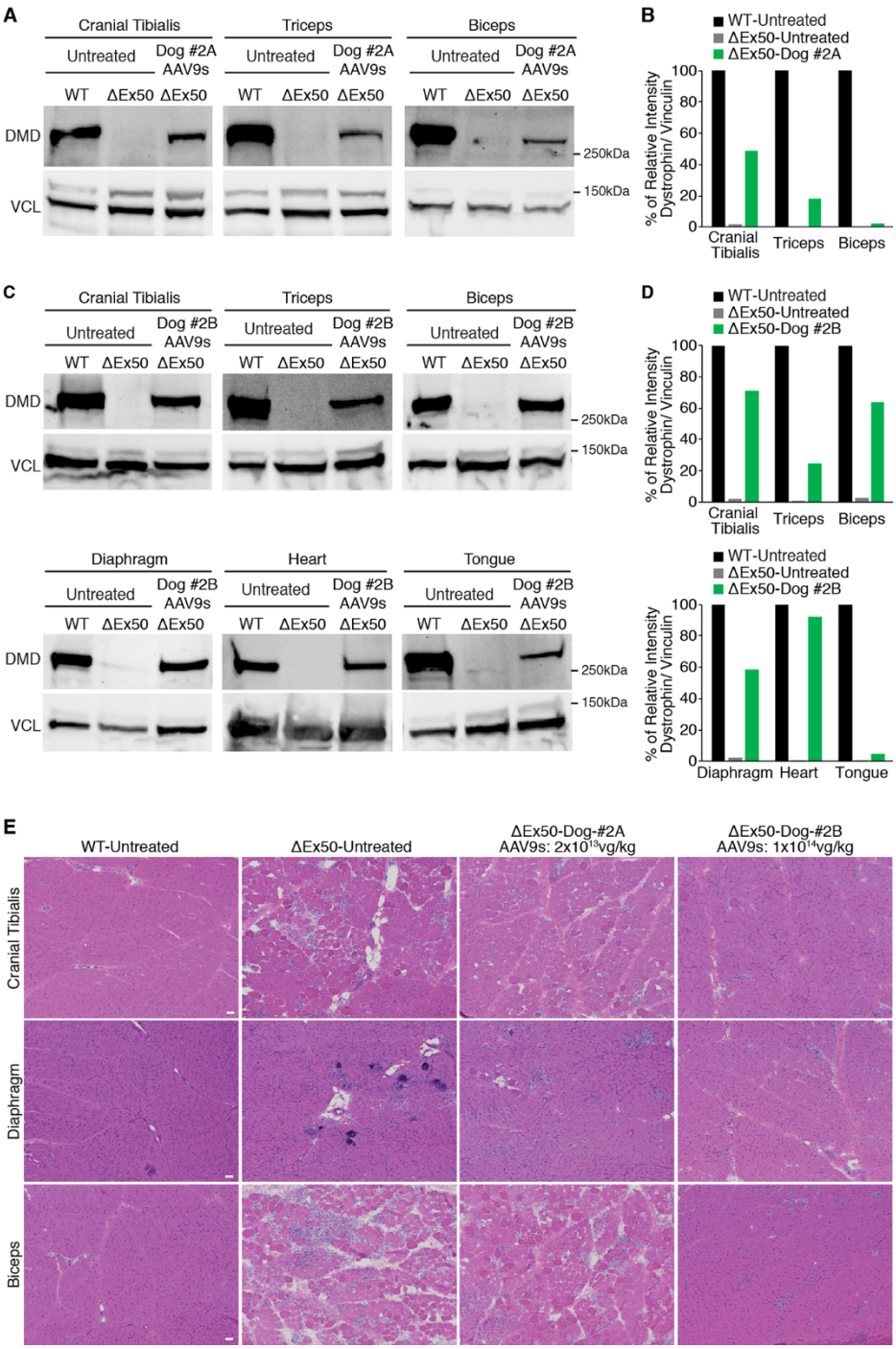

Fig. 4. Western blot of dystrophin and muscle histology following intravenous delivery of AAV9-encoded gene editing components. (**A**) Western blot analysis of dystrophin (DMD) and vinculin (VCL) of cranial tibialis, triceps, biceps muscles of wild type, untreated ΔEx50, and ΔEx50 injected with AAV9-Cas9 and AAV9-sgRNA at $2x10^{13}$ vg/kg for each virus (total virus $4x10^{13}$ vg/kg, referred as ΔEx50-Dog #2A-AAV9s). (**B**) Quantification of dystrophin expression from blots after normalization to vinculin. (**C**) Western blot analysis of dystrophin (DMD) and vinculin (VCL) of cranial tibialis, triceps, biceps, diaphragm, heart, tongue muscles of wild type, untreated ΔEx50, and ΔEx50 injected with AAV9-Cas9 and AAV9-sgRNA at $1x10^{14}$ vg/kg (total virus $2x10^{14}$ vg/kg, referred as ΔEx50-Dog #2B-AAV9s). (**D**) Quantification of dystrophin expression from blots after normalization to vinculin. (**E**) Hematoxylin and eosin (H&E) staining of cranial tibialis, diaphragm and biceps muscles of wild type, untreated ΔEx50, and ΔEx50 injected with AAV9-Cas9 and AAV9-sgRNA at $2x10^{13}$ vg/kg for each virus (total virus $4x10^{13}$ vg/kg) and $1x10^{14}$vg/kg for each virus (total virus $2x10^{14}$ vg/kg). Scale bar: 50μm.

Gene editing restores dystrophin expression in a canine model of Duchenne muscular dystrophy

Leonela Amoasii, John C.W. Hildyard, Hui Li, Efrain Sanchez-Ortiz, Alex Mireault, Daniel Caballero, Rachel Harron, Thaleia-Rengina Stathopoulou, Claire Massey, John M. Shelton, Rhonda Bassel-Duby, Richard J. Piercy and Eric N. Olson

published online August 30, 2018